



## OPEN ACCESS

### EDITED BY

Yinshan Fang,  
Columbia University, United States

### REVIEWED BY

Jing-Zhan Zhang,  
People's Hospital of Xinjiang Uygur  
Autonomous Region, China  
Fenyong Yao,  
University of California, San Diego,  
United States

### \*CORRESPONDENCE

Man S. Kim,  
✉ [manskim@khu.ac.kr](mailto:manskim@khu.ac.kr)  
Soon-Hyo Kwon,  
✉ [soonhyo17@hanmail.net](mailto:soonhyo17@hanmail.net)

†These authors have contributed equally  
to this work

RECEIVED 21 November 2025  
REVISED 06 February 2026  
ACCEPTED 13 February 2026  
PUBLISHED 02 March 2026

### CITATION

Kim S, Lee W, Kim J, Lee Y, Lee K, Kim MS  
and Kwon S-H (2026) Lipid metabolism  
dysregulation in solar lentigo: a multi-  
system-level analysis reveals membrane  
instability and energy  
homeostasis disruption.  
*Front. Cell Dev. Biol.* 14:1751543.  
doi: 10.3389/fcell.2026.1751543

### COPYRIGHT

© 2026 Kim, Lee, Kim, Lee, Lee, Kim and  
Kwon. This is an open-access article  
distributed under the terms of the [Creative  
Commons Attribution License \(CC BY\)](https://creativecommons.org/licenses/by/4.0/).  
The use, distribution or reproduction in  
other forums is permitted, provided the  
original author(s) and the copyright  
owner(s) are credited and that the original  
publication in this journal is cited, in  
accordance with accepted academic  
practice. No use, distribution or  
reproduction is permitted which does not  
comply with these terms.

# Lipid metabolism dysregulation in solar lentigo: a multi-system-level analysis reveals membrane instability and energy homeostasis disruption

Sohyun Kim<sup>1,2†</sup>, Wonmin Lee<sup>1,2†</sup>, Junghyun Kim<sup>3</sup>, Yoonsung Lee<sup>1,2</sup>,  
Kiwon Lee<sup>4</sup>, Man S. Kim<sup>1,2,5\*</sup> and Soon-Hyo Kwon<sup>5,6\*</sup>

<sup>1</sup>Translational-Transdisciplinary Research Center, Clinical Research Institute, Kyung Hee University Hospital at Gangdong, Kyung Hee University College of Medicine, Seoul, Republic of Korea, <sup>2</sup>Department of Medicine, Kyung Hee University College of Medicine, Seoul, Republic of Korea, <sup>3</sup>Division of Tourism & Wellness, Hankuk University of Foreign Studies, Yongin-si, Gyeonggi-do, Republic of Korea, <sup>4</sup>Department of Bioscience and Biotechnology, Hankuk University of Foreign Studies, Yongin-si, Gyeonggi-do, Republic of Korea, <sup>5</sup>Center for Space Biomedical Science, NEXUS Institute, Kyung Hee University, Yongin-si, Republic of Korea, <sup>6</sup>Department of Dermatology, Kyung Hee University Hospital at Gangdong, Kyung Hee University College of Medicine, Seoul, Republic of Korea

Solar lentigo is a common hyperpigmented skin condition caused by chronic ultraviolet exposure, primarily affecting photoaged skin. While previous investigations focused on inflammatory and melanogenic mechanisms, the comprehensive role of lipid metabolism in pathogenesis remains unclear. We aimed to investigate systemic alterations in lipid metabolism and their contribution to solar lentigo development. We performed comprehensive analysis of RNA sequencing data from solar lentigo lesions and control skin samples (n = 7 per group) using metabolic flux simulations, gene co-expression networks, and protein-protein interaction analysis. These multi-system approaches were integrated to identify coordinated alterations in lipid metabolic pathways. Solar lentigo samples exhibited coordinated inhibition of fatty acid elongation, acetyl-CoA carboxylase activity, and sphingolipid biosynthesis, alongside impaired cholesterol synthesis via reduced squalene epoxidase and 7-dehydrocholesterol reductase activity. Compensatory upregulation of phospholipid synthesis enzymes and dihydroceramide desaturases was observed. Pathway disruption and altered calcium signaling, indicating aberrant cellular energy metabolism and membrane integrity. These findings suggest that solar lentigo pathogenesis involves systematic lipid metabolism dysregulation beyond melanogenesis, potentially contributing to membrane instability, energy homeostasis disruption and redox imbalance. The identification of specific metabolic bottlenecks reveals novel targets for lipid-based therapeutic approaches in pigmentary diseases.

### KEYWORDS

fatty acid elongation, lipid metabolism, metabolic flux simulation, oxidative stress, solar lentigo, sphingolipid metabolism

## 1 Introduction

Solar lentigo (SL) is a hyperpigmented skin disorder primarily affecting middle-aged and elderly individuals. It manifests as well-defined light-to-dark brown spots commonly located on skin areas with prolonged exposure to ultraviolet (UV) radiation, such as the face. Chronic UV exposure is identified as the main etiological factor in the development of SL (Bastiaens et al., 2004), leading to localized increases in melanin synthesis and alterations in both epidermal and dermal structures (Yonei et al., 2012). Given its strong correlation with photoaging and its impact on aesthetics, significant research efforts have been directed towards understanding the pathophysiological mechanisms underlying SL and exploring effective therapeutic strategies.

Many studies have emphasized the changes in metabolic and gene expression profiles in SL, particularly focusing on alterations in inflammatory gene expression. DNA microarray analyses have revealed the upregulation of genes associated with inflammation in SL lesions, including six genes specifically associated with the inflammatory response, highlighting the significance of microinflammation in photoaged skin (Goyarts et al., 2007). Also, other studies have shown an increased expression of genes involved in both inflammation and fatty acid metabolism in SL (Aoki et al., 2007). These molecular findings offer valuable insights into the pathological features of SL and shed light on the intricate interplay between inflammation and metabolism during SL development.

However, the precise role of lipid metabolism in the SL remains unclear. Although lipid metabolism is recognized as a critical factor in the pathogenesis of various skin conditions (Pietrzak et al., 2010; Kang et al., 2011; Ewald et al., 2015), its involvement in SL has thus far only been suggested indirectly. Studies have reported an increased expression of endothelin-1 and endothelin B receptors in the lesional epidermis (Imokawa, 2019). Although these studies did not explicitly focus on lipid metabolism, endothelin-1 is known to influence lipid metabolism by reducing the uptake of long-chain fatty acids, indicating a potential link between these factors and lipid metabolism in SL (Chien et al., 2011).

Metabolic flux simulations have recently provided innovative insights into disease studies that were previously unexplored (Smith and Robinson, 2011; Batagov et al., 2023). To date, previous studies on SL have mainly focused on analyzing gene or protein expression levels in isolation (Goyarts et al., 2007; Aoki et al., 2007; Motokawa et al., 2005). While investigations into the regulation of inflammation and oxidative stress responses in SL have been conducted, studies utilizing a multi-system-level approach remain relatively limited (Jeong et al., 2024). A recent integrative study by Cai et al. (2025) employed dynamic network driver analysis to identify key regulatory modules in SL, providing a novel perspective on its molecular pathology (Cai et al., 2025). However, comprehensive metabolic flux analysis combined with transcriptomic profiling has not been previously applied to understand the metabolic dysregulation in SL pathogenesis. This study aimed to assess the impact of lipid metabolism in SL using a multi-systemic strategy incorporating differential gene expression patterns, protein-protein interactions, and alterations in metabolic reaction activities.

## 2 Materials and methods

### 2.1 Patient samples and RNA-seq processing

This study utilized SL skin samples that we previously collected from seven patients at Kyung Hee University Hospital at Gangdong, where all procedures were approved by the local Institutional Review Board (IRB). Written informed consent was obtained from all participants prior to sample collection, and the study was conducted in full accordance with the ethical principles for research involving human subjects. Paired skin samples (5 mm diameter) were collected from the SL and adjacent normal skin of seven patients at Kyung Hee University Hospital at Gangdong. The mean age was  $82.0 \pm 10.2$  years (range, 67–96 years). The locations were on the chin (71.4%), cheek (14.3%), and temple (14.3%). Generation of raw sequencing data and subsequent bioinformatic processing were conducted according to our previously published methods (Choi et al., 2025). Key processing steps included read alignment to the human reference genome (GRCh38) and normalization of transcript expression to transcripts per million (TPM) for all downstream analyses.

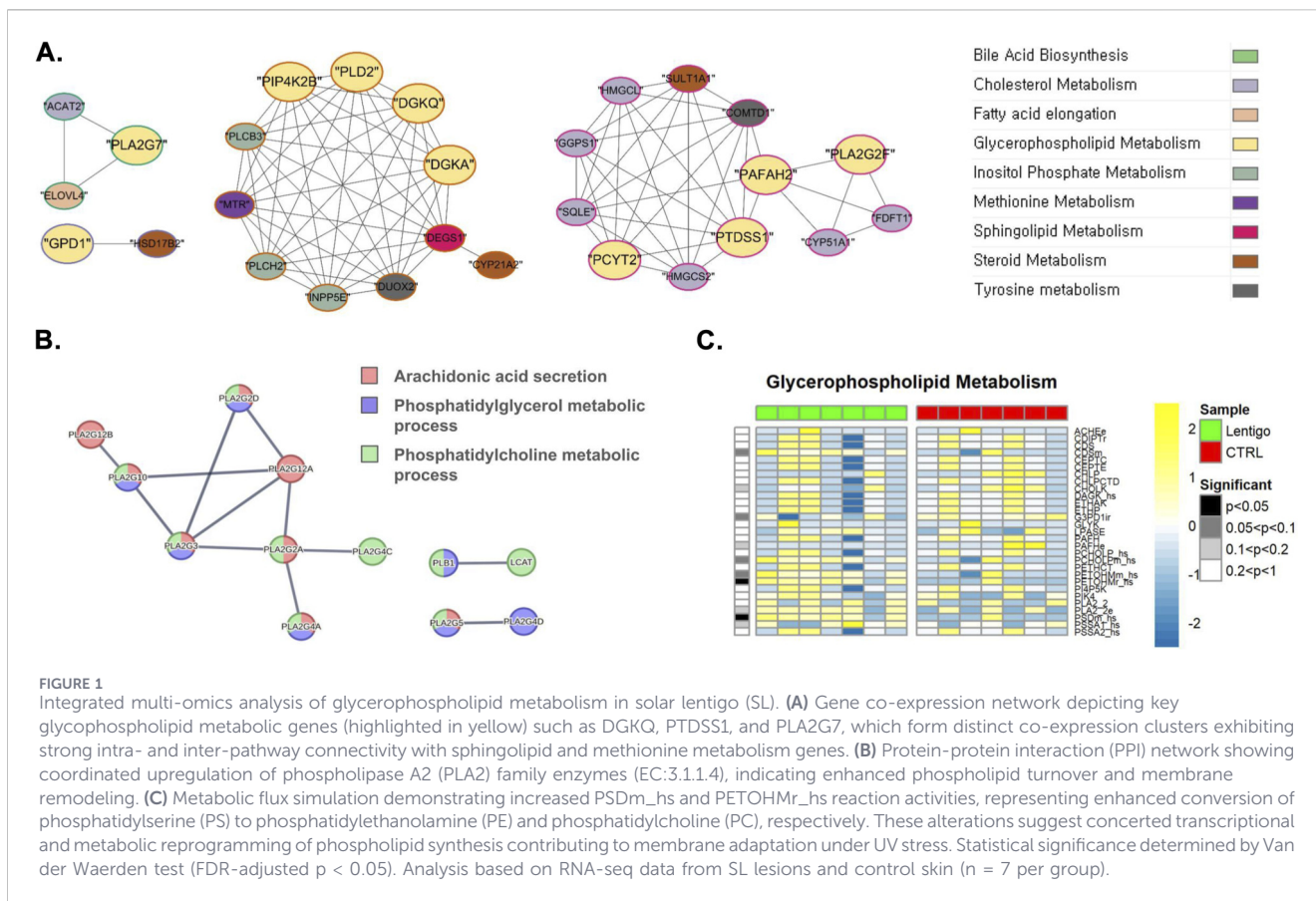
### 2.2 Expression profiling and pathway enrichment assessment

Differential expression analysis between SL and control samples ( $n = 7$  per group) was performed on the raw count matrix using the DESeq2 package (v1.48.0) in R. Genes were considered significantly differentially expressed if they met a False Discovery Rate (FDR) adjusted  $p$ -value  $< 0.05$  and an absolute  $\log_2$  fold change  $> 0.01$ .

Functional annotation of differentially expressed genes was conducted through Gene Ontology (GO) term enrichment using the clusterProfiler R package (v4.16.0) (Wu et al., 2021). To examine pathway-level changes, Gene Set Enrichment Analysis (GSEA) was applied using pre-ranked gene lists ordered by  $\log_2$  fold change values, implemented through the fGSEA R package (v1.24.0) (Korotkevich et al., 2016). Metabolic and signaling pathway analysis was performed using KEGG database annotations via the gage package (v2.58.0). Statistical significance for all enrichment tests was set at FDR-adjusted  $p$ -value  $< 0.05$ . Protein interaction networks were constructed by querying the STRING database (v12.0) (Szklarczyk et al., 2023) with the differentially expressed gene set. Network topology analysis and visualization were subsequently performed using Cytoscape (v3.10.3) (Shannon et al., 2003). Functional annotation enrichment analysis was conducted for each PPI network using Gene Ontology biological process terms to elucidate pathway-specific molecular functions.

### 2.3 Clustering analysis

To identify stable gene clusters based on co-expression patterns, consensus clustering was performed on the subset of genes related to the predefined metabolic pathways using the ConsensusClusterPlus (v1.64.0) package in R. The  $\log_2$  fold change values for these genes were used as the input data matrix. Prior to clustering, the data was centered by the median of each gene. The  $k$ -means algorithm with Euclidean distance was applied for clustering. The analysis was repeated 30 times, and the number of clusters ( $k$ ) was evaluated



across a range from 2 to 10 to ensure the stability of the clustering results. The consensus matrix, generated from this analysis, served as a measure of co-expression similarity between all gene pairs.

Genes associated with energy metabolism were selected based on the model's gene-reaction annotation framework, followed by differential expression analysis using the DESeq2 R package (v1.48.0). Expression pattern-based clustering of differentially expressed genes was executed using the ConsensusClusterPlus R package. The K-means clustering algorithm implemented in ConsensusClusterPlus facilitated the identification of distinct gene expression clusters and enabled the characterization of potential molecular subtypes within the dataset.

## 2.4 Metabolic flux analysis

To simulate cellular metabolism alterations, we employed the custom, constraint-based flux simulation previously developed by our group using the Recon1 genome-scale model (da Silveira et al., 2020; Guarnieri et al., 2023; Duarte et al., 2007). The simulation was governed by two primary constraints: first, corresponding enzyme expression levels were used to set the bounds for reaction fluxes, and second, main energy-associated pathways were set to maximal optimization (specifically, Citric Acid Cycle, Oxidative Phosphorylation, CoA Synthesis, CoA Catabolism, Glycolysis and Gluconeogenesis, NAD Metabolism, Fatty Acid Synthesis, Fatty Acid Oxidation, and Biomass and Maintenance Functions). The Van der Waerden (VdW) test was then used to quantify the resulting metabolic alterations between the two conditions. Metabolic flux

simulations utilized reaction identifiers from the BiGG Models database (<http://bigg.ucsd.edu/>).

## 3 Results

### 3.1 Glycerophospholipid dysregulation and membrane composition changes in solar lentigo

In the context of SL, our analysis revealed considerable upregulation of critical phospholipid synthesis reactions. At the transcriptional level, gene co-expression network analysis (Figure 1A) revealed significant regulatory interconnections among key genes involved in glycerophospholipid metabolism. As shown in Figure 1A, these genes (highlighted in yellow), such as *DGKQ*, *PTDSS1*, and *PLA2G7*, anchored to distinct co-expression clusters that demonstrated strong intra-pathway co-regulation and significant inter-pathway co-expression. Major glycerophospholipid gene clusters centered around *DGKQ* (closely co-expressed with other glycerophospholipid enzymes such as *PLD2*) and *PTDSS1* (co-expressed with *PFAFH2*) showed robust connections to genes involved in sphingolipid metabolism (*DEGS1*) and methionine metabolism. Additionally, *PLA2G7* exhibited co-expression with genes integral to cholesterol metabolism (*ACAT2*) and fatty acid elongation (*ELOVL*). This intricate network view underscores extensive crosstalk with other critical lipid pathways and supports the observed upregulation of phospholipid metabolic processes in the SL.



FIGURE 2

Integrated multi-omics analysis of fatty acid elongation in solar lentigo (SL). (A) Gene network analysis highlighting connections between ELOVL4, PLA2G7, and ACAT2, showing coordinated regulation between fatty acid elongation, phospholipid metabolism, and cholesterol synthesis. (B) PPI network demonstrating downregulation of ACACA, ACACB, ACSBG1, and ACSL5, which form a module involved in acyl-CoA biosynthesis, suggesting impaired fatty acid activation. (C) Metabolic flux simulation reveals decreased FAEL183 and DESAT18\_3 reaction activity, indicating impaired elongation and desaturation of long-chain fatty acids, which may compromise membrane fluidity and energy balance. Statistical significance determined by Van der Waerden test (FDR-adjusted  $p < 0.05$ ). Analysis based on RNA-seq data from SL lesions and control skin ( $n = 7$  per group).

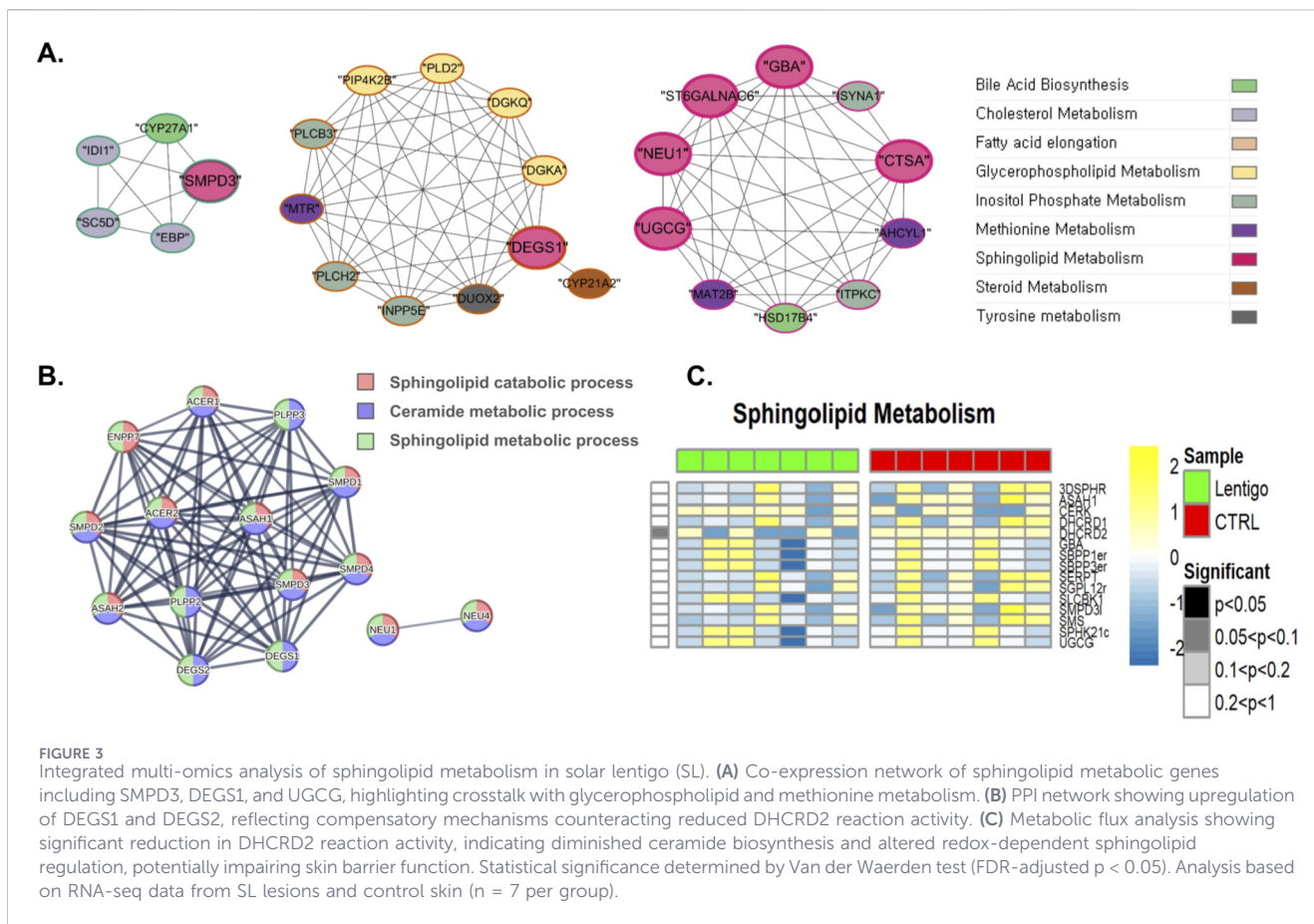
Supporting these transcriptional findings, protein-protein interaction (PPI) analysis (Figure 1B; Supplementary Figure S1) demonstrated functional clustering among PLA2 family enzymes (EC:3.1.1.4), including PLA2G10, PLA2G2D, PLA2G3, PLA2G2A, PLA2G4C, PLA2G4A, and PLA2G5, which facilitate arachidonic acid release from phosphatidylcholine. These protein-protein interaction patterns reinforce the coordinated regulation of phospholipid metabolic machinery.

At the metabolic level, flux simulations of the glycerophospholipid pathway (Figure 1C) demonstrated these transcriptional changes translate into functional metabolic alterations. We observed a pronounced increase in Phosphatidylserine decarboxylase reaction (BiGG ID: PSDm\_hs) activity, which converts phosphatidylserine (PS) into phosphatidylethanolamine (PE). PE serves as an essential phospholipid that contributes to membrane integrity and stabilization of mitochondrial proteins. Furthermore, substantial upregulation of the PETHMr\_hs reaction was detected, catalyzed by phosphatidylethanolamine N-methyltransferase. This process involves the methylation of phosphatidylethanolamine to produce phosphatidylcholine (PC), utilizing S-adenosylmethionine as a methyl donor and yielding S-adenosylhomocysteine as a byproduct. Given that phosphatidylcholine is a predominant membrane component vital for lipid homeostasis and signaling, its increased synthesis in the SL suggests concerted modifications in membrane phospholipid composition that align with the observed transcriptional regulatory networks.

As shown in Figure 2C, our metabolic flux simulation of fatty acid metabolism in the SL revealed a substantial downregulation of

the stearoyl-CoA desaturase reaction (BiGG ID: DESAT18\_3), suggesting impaired fatty acid desaturation and elongation processes that may alter membrane rigidity. This reaction converts stearoyl-CoA to oleoyl-CoA. Stearoyl-CoA desaturase is critical for fatty acid desaturation, an essential process for maintaining lipid composition and membrane fluidity (Ntambi, 1999). Another reaction, dihydroceramide desaturase reaction (BiGG ID: DHCRD2), of the sphingolipid pathway showed a predominant reduction in SL, where the reduction in the activity of dihydroceramide desaturase led to a decline in ceramide production (Figure 3C). Dihydroceramide desaturase plays a pivotal role in the enzymatic conversion of dihydroceramide to ceramide, which is crucial for maintaining the equilibrium between sphingolipids and dihydro-sphingolipids. In contrast, the upregulation identified through PPI analyses can be attributed to the increased transcription and translation of dihydroceramide desaturase, which serves as a compensatory mechanism for diminished DHCRD2 reaction. As shown in Figure 3B (see also Supplementary Figure S2), our PPI analysis revealed the upregulation of DEGS1 and DEGS2, both annotated as EC: 1.14.19.17 and EC:1.14.18.5, respectively, in the KEGG database. These enzymes likely function in compensatory mechanisms to mitigate the reduced activity of dihydroceramide desaturase, thereby preserving cellular homeostasis. Such compensatory responses are frequently observed in patients with dermatological disorders (Coelho et al., 2015).

The complex interplay within the lipid metabolism was further illustrated by gene network analyses, as shown in Figure 2A (fatty acids) and Figure 3A (sphingolipids). Figure 2A shows that

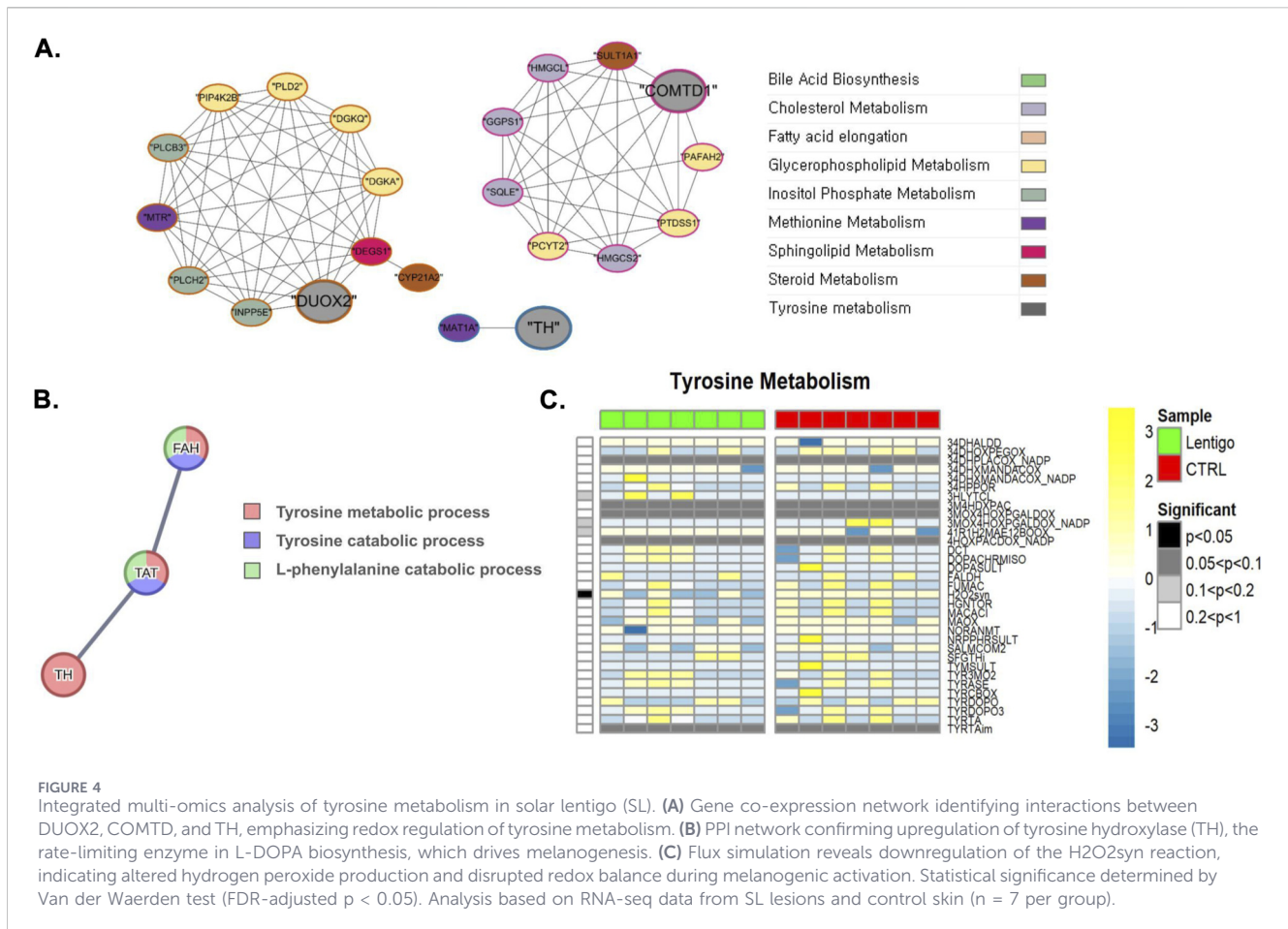


ELOVL4, crucial for the synthesis of very long-chain fatty acids (VLCFAs) necessary for ceramide production, is connected to *PLA2G7*, a gene related to glycerophospholipid metabolism, and *ACAT2*, a gene related to cholesterol metabolism. **Figure 3A** depicts a broader network, particularly within sphingolipid metabolism, which includes interactions involving *SMPD3* (involved in ceramide generation), *DEGS1* (dihydroceramide desaturase, critical for synthesizing ceramide from dihydroceramide), and *UGCG* (which utilizes ceramide), along with their connections to genes involved in other lipid pathways. These network analysis results collectively highlight the integrated regulation of pathways essential for maintaining sphingolipid homeostasis and membrane integrity in SL.

### 3.2 Disruption of oxidative stress management

Having recognized that oxidative stress disrupts the balance of the cellular redox state, affecting homeostasis and cellular responses in the SL, our analysis of sphingolipid metabolism revealed a predominant downregulation of the DHCRD2 reaction in the SL (**Figure 3C**). This reaction relies on FADH2 as a cofactor, and its enzymatic function is influenced by the presence of O<sub>2</sub> and NAD(P)H. These observations highlight the bidirectional interactions between the cellular redox environment and dihydroceramide desaturase activity (Fabrias et al., 2012). Similarly, in tyrosine

metabolism, SL samples displayed a substantial downregulation of the hydrogen peroxide synthesis reaction (BiGG ID: H2O2syn), where the reaction is facilitated by the enzyme hydrogen peroxide synthase, which is dependent on NADPH, and converts oxygen (O<sub>2</sub>), NADPH, and protons (H<sup>+</sup>) into hydrogen peroxide (H<sub>2</sub>O<sub>2</sub>) and NADP<sup>+</sup> (**Figure 4C**). Hydrogen peroxide is essential for modulating the cellular redox state and functions as a signaling molecule that is critical for preserving homeostasis and cellular responses. Further insights into these metabolic shifts were provided by network analysis (**Figures 3A, 4A**). The sphingolipid network analysis (**Figure 3A**), consistent with the alterations in dihydroceramide desaturase activity, reaffirmed the complex regulatory interactions among the key enzymes governing ceramide synthesis and turnover. More pertinent to the changes in tyrosine metabolism, **Figure 4A** depicts interactions involving *DUOX2* (relevant to H<sub>2</sub>O<sub>2</sub> balance) and *COMTD* (linked to L-DOPA metabolism), and importantly, visualized tyrosine hydroxylase (*TH*), the pivotal enzyme for L-DOPA production from tyrosine. PPI analysis further supported this upregulation by revealing increased translation of the *TH* gene (EC:1.14.16.2), highlighting its enhanced role in tyrosine metabolism, as shown in **Figure 4B** and **Supplementary Figure S3**. Increased tyrosine hydroxylase activity promoted melanogenesis, resulting in increased the production of reactive oxygen species (ROS) (Iyengar and Misra, 1987). These observations suggest that tyrosine metabolism plays a significant role in the management of oxidative stress in SL.



### 3.3 PTEN-mediated PI3K/Akt pathway disruption and calcium homeostasis alterations

As illustrated in Figure 5C, our metabolic simulation analysis exhibited a considerable reduction in the PI(3,4,5)P<sub>3</sub> phosphatase reaction (BiGG ID: PI345P3Pn) in SL, where the reaction is facilitated by phosphatidylinositol-3,4,5-trisphosphate 3-phosphatase, an enzyme encoded by the *PTEN* gene. *PTEN* is integral to the regulation of a variety of cellular processes, including cell metabolism, by modulating Akt activity via the PTEN/PI3K/Akt signaling pathway (Downward, 2004). Further insights at the network level were provided by gene coexpression analysis (Figure 5A). This analysis highlights the key enzymes within inositol phosphate metabolism (greyish-green nodes) and their interactions. Notably, *INPP5E*, an inositol polyphosphate-5-phosphatase involved in modulating PI3K/Akt signaling by regulating PIP levels, is part of a large cluster interconnected with glycerophospholipid (e.g., *PLCB3*) and sphingolipid metabolism genes. The network also prominently featured enzymes critical for calcium signaling. Phospholipase C isoforms, such as *PLCB3* (a key generator of IP<sub>3</sub> and diacylglycerol (DAG) from PIP<sub>2</sub>) and *PLCH2*, formed a module. In contrast, *ITPKC* (inositol-trisphosphate 3-kinase), which influences IP<sub>3</sub> levels and calcium signals, was observed in a separate cluster interacting with sphingolipid and methionine metabolism genes. These visualized

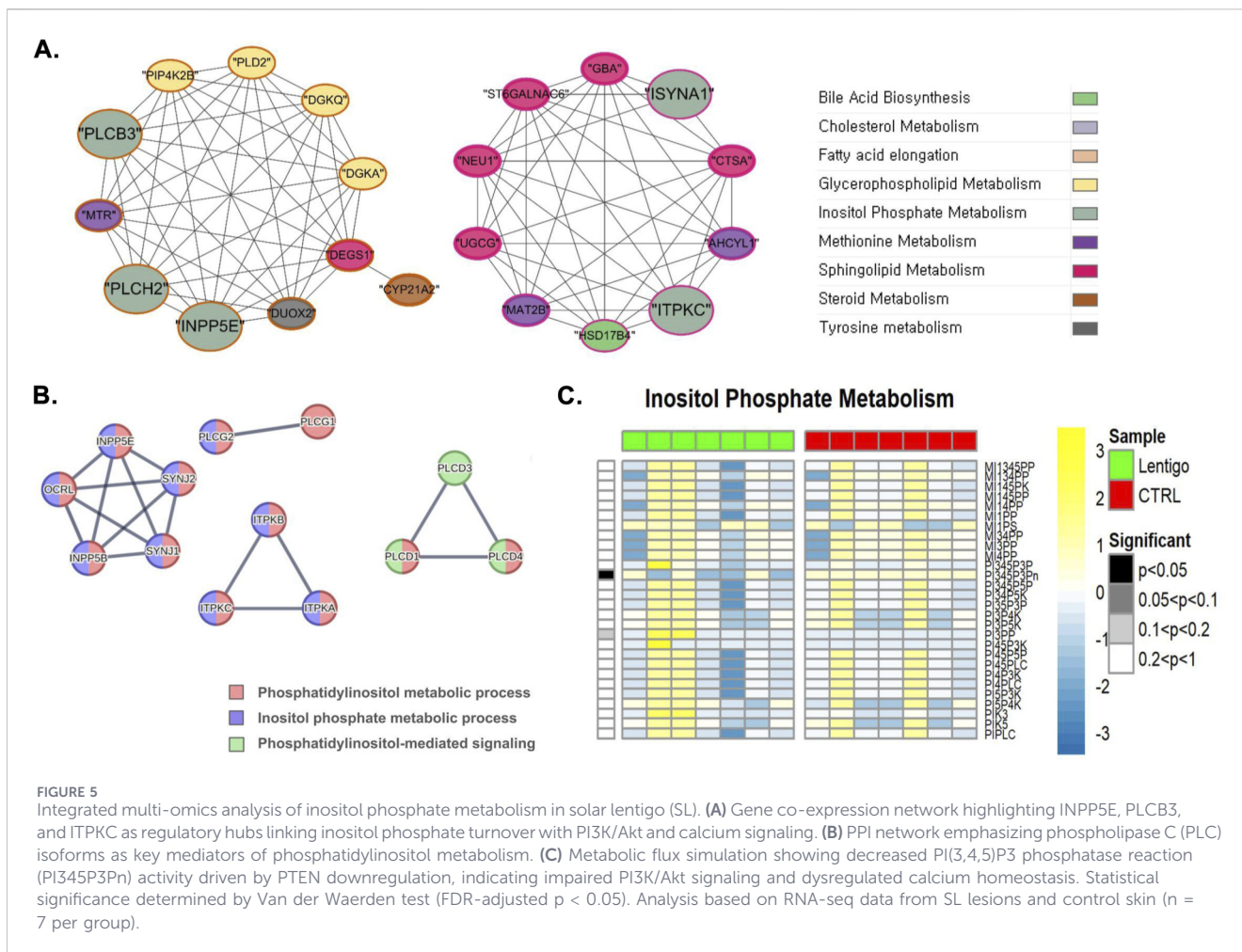
networks underscore the complex interplay and co-regulation of proteins involved in both PI3K/Akt pathway modulation and calcium signaling through inositol phosphates.

### 3.4 Impaired fatty acid elongation and energy metabolism in solar lentigo

In SL samples, membrane fluidity maintenance and fatty acid elongation were predominantly inhibited. In the context of fatty acid metabolism, pronounced reduction of the fatty-acyl-CoA elongation reaction (BiGG ID: FAEL183) was observed, indicating a decrease in the elongation activity of fatty acids (Figure 2C). This reaction, catalyzed by a fatty-acyl-CoA elongation enzyme, converts linoleoyl-CoA to dihomoy-linolenoyl-CoA using malonyl-CoA as a substrate.

Additionally, *ACACA* and *ACACB* (EC:6.4.1.2), which convert acetyl-CoA to malonyl-CoA, showed suppressed expression in SL (Supplementary Figure S4). Malonyl-CoA not only acts as a key substrate for fatty acid elongation but also serves as a regulatory molecule for fatty acid oxidation (Bowman and Wolfgang, 2019). Therefore, a decreased activity of these enzymes is likely to impair both processes.

PPI analysis, as shown in Figure 2B, supported this observation by revealing that *ACACA*, *ACACB*, and multiple long-chain acyl-CoA synthetases, such as *ACSBG1* and *ACSL5*, form a closely connected module within the acyl-CoA biosynthetic process. These enzymes, many of which were downregulated, are central



to fatty acid activation, further supporting the functional suppression of SL.

Similarly, disruption of bile acid metabolism was observed. Figure 6A shows that CYP27A1, AMACR, and HSD17B4, which are essential enzymes in bile acid biosynthesis, exhibited notable interactions with genes involved in cholesterol and sphingolipid metabolism. This network suggests that bile acid metabolism does not operate in isolation but rather interfaces with broader lipid regulatory pathways.

Additionally, Figure 6B and Supplementary Figure S5 show the coordinated suppression of CH25H (EC:1.14.99.38), CYP27A1 (EC:1.14.15.15), and AMACR (EC:5.1.99.4), which act sequentially during bile acid biosynthesis. This pattern implies multi-step disruption of the pathway and potential downstream effects on cholesterol turnover.

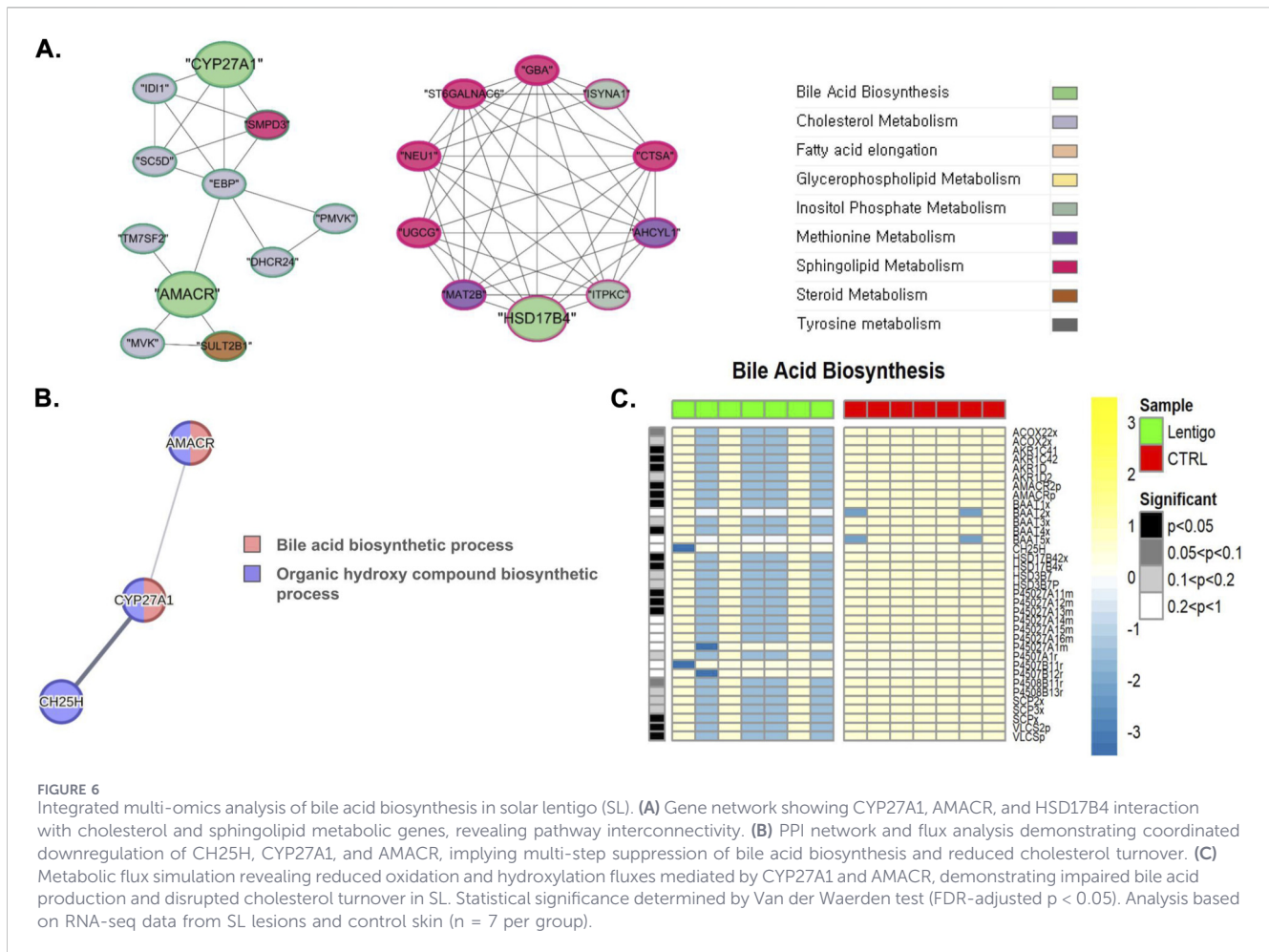
Collectively, these findings indicate that SL is characterized by broad dysregulation of fatty acid metabolism, encompassing elongation, activation, and oxidation, likely leading to altered lipid composition and signaling.

### 3.5 Cholesterol biosynthesis modification and sterol homeostasis dysfunction

Figure 7C shows a substantial downregulation of key cholesterol biosynthesis reactions in SL. Specifically, the squalene synthase

reaction (BiGG ID: SQLSr) and squalene epoxidase endoplasmic reticular NADP reaction (BiGG ID: SQLER) were diminished, indicating a decreased conversion of farnesyl pyrophosphate to squalene, and subsequently, squalene to 2,3-oxidosqualene. Squalene epoxidase (SQLE) is responsible for the stereospecific conversion of squalene to 2,3(S)-oxidosqualene, which is the initial oxygenation step in cholesterol biosynthesis. Its downregulation may hinder cholesterol synthesis and disturb cholesterol homeostasis (Padyana et al., 2019). In addition, DHCR71r reaction, DHCR72r reaction, DHCR241r reaction, DHCR242r reaction, and DHCR243r reaction, which are catalyzed by 7-dehydrocholesterol reductase and 24-dehydrocholesterol reductase, were reduced. These reactions are pivotal in the terminal phases of cholesterol biosynthesis and facilitate the conversion of 7-dehydrocholesterol and desmosterol to cholesterol. As shown in Figure 7A, gene network analysis further underscored the coordinated nature of cholesterol metabolism. This analysis revealed distinct clusters of functionally associated genes central to cholesterol biosynthesis (nodes predominantly colored light gray), including key enzymes, such as *TM7SF2* (DHCR7), *DHCR24*, *MVK*, *PMVK*, and *CYP51A1*. These clusters demonstrate their interconnectedness within the cholesterol synthesis pathway and their links to other lipid metabolic processes, such as sphingolipid and bile acid biosynthesis.

Translation-level analysis indicated a considerable reduction in the levels of critical proteins involved in cholesterol transport, as shown in



**Supplementary Figure S6.** Complementing these findings, PPI analysis was performed to elucidate the interaction networks of these key cholesterol transport-related proteins (Figure 7B). This network highlighted *LDLR*, *LRP1*, and *LRP2* receptors crucial for LDL uptake and their association with amyloid-beta and plasma lipoprotein particle clearance (nodes colored blue and/or green, reflecting their pathway involvement). The same PPI network underscored the centrality of *APOA1*, the main high-density lipoprotein (HDL), in the regulation of plasma lipoprotein levels and Plasma lipoprotein particle clearance (red and/or green nodes). The observed downregulation of these interconnected proteins, *LDLR* and *LRPs* for LDL uptake, and *APOA1* for HDL formation and reverse cholesterol transport, significantly impaired cholesterol homeostasis. For instance, diminished *APOA1* impairs HDL formation, reduces cholesterol efflux from peripheral tissues to the liver, leads to lipid dysregulation, and diminishes the ability of HDL to modulate immune cell function, potentially worsening inflammatory and autoimmune conditions (Trakaki and Marsche, 2020).

## 4 Discussion

Lipid metabolism and the cellular redox state are intimately linked by multiple biochemical processes that are relevant to the pathophysiology of SL. The changes in sphingolipid and tyrosine

metabolism described above imply a complex interplay between lipid dysregulation and redox modulation of oxidative stress in diseased UV skin.

Reduction of the response of *DHCRD2* reactions to sphingolipid metabolism results in loss of redox balance in SL lesions. Dihydroceramide desaturase activity is dependent on *FADH2* cofactor,  $O_2$  availability, and *NAD(P)H*, setting up a dynamic interaction between cellular redox state and sphingolipid homeostasis (Fabrias et al., 2012; Łuczaj et al., 2020). Sphingolipid metabolism is critical for the resistance of cells to oxidative stress because sphingolipid-preserving enzymes, such as *CERKL*, have been shown to protect skin cells from oxidative damage and maintain ceramide synthesis under stress conditions (Meyer et al., 2021; Dini et al., 2021). The inhibition of *DHCRD2* reaction may compromise the antioxidant protective mechanisms of the skin, potentially increasing UV-induced cell damage.

Network analysis of the interactions between *COMTD1*, *DUOX2*, and *TH* revealed complex redox regulation in SL. *DUOX2*, which maintains the balance of hydrogen peroxide, appears to be coordinately regulated by the induction of *TH* (Kumar et al., 2018). *TH* activity activated by enhancement of PPI analysis for enhanced gene translation promotes L-DOPA formation from tyrosine required for melanogenesis, but simultaneously produces reactive oxygen species (ROS) (Li et al.,



et al., 2018). However, this compensation appears insufficient, as ceramide deficiency remains a characteristic feature of aged and photodamaged skin. The inability to fully restore ceramide levels may explain the compromised barrier function and increased susceptibility to environmental stressors observed in solar lentigines (Ma et al., 2020).

Overexpression of PLA2 family enzymes indicates active phospholipid turnover and membrane remodeling in SL. While potentially contributing to inflammatory signaling, this increased PLA2 activity may also represent an attempt to remodel damaged membrane components and facilitate cellular repair processes (Dalmau et al., 2018). The central role of PLA2G7 as a regulatory hub connecting glycerophospholipid, cholesterol, and fatty acid metabolism suggests that SL represents a systemic reorganization of membrane metabolism rather than isolated pathway disruption.

Impairment of cholesterol biosynthesis through reduced SQLE, DHCR7, and DHCR24 activity disrupts this essential barrier component. Cholesterol plays a crucial role in skin barrier formation and keratinocyte differentiation and its synthesis is tightly regulated by sterol regulatory element-binding proteins (Wang et al., 2020). Coordinated downregulation of cholesterol transport proteins LDLR, LRP1, LRP2, and APOA1 further exacerbates cholesterol deficiency in SL lesions, compromising membrane structure and barrier integrity (Muresan et al., 2019). This cholesterol dysregulation may contribute to altered membrane fluidity and compromised intercellular communication between keratinocytes and melanocytes, potentially influencing the characteristic hyperpigmentation pattern of solar lentigines.

The overall dysregulation of fatty acid metabolism in SL represents a fundamental alteration in cellular energy homeostasis, which is more than simply pigmentation. The drastic reduction of the FAEL183 reaction defines impairment in conversion of linoleoyl-CoA to dihomo- $\gamma$ -linolenoyl-CoA, disrupting very-long-chain fatty acid synthesis required for cellular energy production and membrane integrity (Oh et al., 2022).

The interaction network between ELOVL4, PLA2G7, and ACAT2 demonstrates the coordinated regulation of fatty acid elongation with phospholipid and cholesterol metabolism. The cross-talk suggests that SL involves the synchronized disruption of multiple lipid biosynthetic pathways essential for maintaining cellular energy homeostasis (Luo et al., 2020).

The suppressed expression of ACACA and ACACB is the primary bottleneck in cellular energy metabolism. Both enzymes catalyze acetyl-CoA to malonyl-CoA, which is not only the immediate substrate for the elongation of fatty acids but also a primary regulatory molecule suppressing the oxidation of fatty acids (Tu et al., 2024). The dual role of malonyl-CoA is that reduced ACACA/ACACB activity has a cascade effect, both suppressing fatty acid synthesis and disrupting the balance between lipid anabolism and catabolism, with the ultimate effect of sabotaging cellular energy production (Papaccio et al., 2024).

Protein-protein interaction analysis showed that a tightly connected module of ACACA, ACACB, and various long-chain acyl-CoA synthetases (ACSBG1 and ACSL5) underscores the concertedness of fatty acid activation defects in SL. All these enzymes play critical roles in conjugating fatty acids to energy-rich acyl-CoA derivatives for cellular metabolism. Coordinated downregulation of this enzyme module shows that SL lesions

experience a systematic disruption of fatty acid utilization, potentially leading to energy deficiency and cellular dysfunction (Yu et al., 2024).

In the pathogenesis of SL, changes in fatty acid metabolism can exert profound effects on energy homeostasis and pigment production in melanocytes. Fatty acid metabolism provides the energy substrates required for melanogenesis and melanosome transport (Chen X. et al., 2024). The disruption noted in fatty acid synthesis and activation can therefore contribute to the metabolic dysregulation that characterizes solar lentigines (Li et al., 2025).

Extreme repression of bile acid synthesis, as indicated by the downregulation of CYP27A1 and AMACR, is another facet of metabolic failure in SL. Their repression in a coordinated manner indicates multi-step disruption that can lead to cholesterol accumulation and deranged energy metabolism. Such coordinated disruption of both fatty acid and bile acid metabolism is reflective of a fundamental change in energy homeostasis that may be implicated in UV-induced skin aging pathophysiology.

Simulation analysis of metabolic flux showed multifaceted dysregulation of the PI3K/Akt pathway in SL, where PTEN, an important tumor suppressor that is commonly mutated in most skin cancers, such as melanoma (Sun et al., 2024; Chen et al., 2021), was mostly downregulated. PTEN functions as a suppressive modulator of the PI3K/Akt signaling pathway by dephosphorylation of PIP<sub>3</sub> to PIP<sub>2</sub>, and its suppression results in the constitutive activation of downstream oncogenic pathways that have been implicated in various dermatological conditions like acne, psoriasis, and skin cancers (Lee et al., 2021; Namiki et al., 2015).

Gene coexpression network analysis identified INPP5E, an inositol polyphosphate-5-phosphatase, as a regulatory hub node in a large interconnected cluster. INPP5E controls PI3K/Akt signaling by modulating phosphoinositide levels and network integration with glycerophospholipid metabolism genes, suggesting coordinated regulation of lipid signaling pathways in SL pathogenesis (Scortegagna et al., 2015). The upregulated INPP5E activity in SL is a compensatory mechanism that phosphorylates PIP<sub>3</sub> into PIP<sub>2</sub>, thereby conferring tumor-suppressing activities as observed in melanoma, where enzymatic activity is used to curtail malignant transformation (Conde-Perez et al., 2015) (Supplementary Figure S7).

Network analysis also focused on the central role of the PLC isoforms PLCB3 and PLCH2, which are unique functional modules in the co-expression network. The activation of PLC consumes PIP<sub>2</sub> to generate inositol 1,4,5-trisphosphate (IP<sub>3</sub>) and DAG, which may reduce the level of PIP<sub>3</sub> and indirectly suppress PI3K/Akt signaling. This double mechanism—direct dephosphorylation of PIP<sub>3</sub> by phosphatases and indirect reduction through PLC consumption of PIP<sub>2</sub>—defines a coordinated inhibition of pro-proliferative signaling in SL lesions.

Calcium signaling is another major parallel pathway affected in SL, with deep alterations in intracellular calcium homeostasis-regulating enzymes. Activation of the observed PLC and network positioning of ITPKC (inositol-trisphosphate 3-kinase) within a separate cluster that is in contact with sphingolipid and methionine metabolism genes indicates a very complex regulatory network controlling IP<sub>3</sub> concentration and subsequent intracellular calcium release. In melanocytes, PLC plays a central

role in UV light detection and cellular response signaling pathways (Wang et al., 2021), whereas calcium signaling is essential for UV-stimulated melanogenesis and subsequent melanin transfer to keratinocytes (Luo et al., 2023b).

The disruption of calcium homeostasis in the SL is of particular significance owing to its double biological function. In healthy individuals, controlled calcium signaling enhances melanogenesis via tyrosinase activation and melanosome transport (Luo et al., 2023b). However, in the context of chronic UV exposure, a characteristic of SL development, hypercalcemic influx could trigger oxidative stress mechanisms and participate in the pathological pigmentation patterns of such lesions (Kim and Lee, 2023). The network-based identification of ITPKC within a metabolically distinct cluster suggests a putative regulatory function in calcium signaling, which may be impaired in SL, possibly leading to dysregulated IP<sub>3</sub> turnover and altered calcium dynamics.

The intersection of these findings indicates that SL pathogenesis represents a synergistic dysregulation of both the PI3K/Akt and calcium signaling pathways by virtue of the complex interactions between phosphoinositide metabolism, PLC activation, and inositol phosphate regulatory enzymes.

This comprehensive discussion of multi-systemic dysregulation reveals that SL pathogenesis is an orchestrated dysregulation of lipid metabolism beyond melanin overproduction, including orchestrated dysregulation of fatty acid elongation, sphingolipid homeostasis, and membrane structure. Downregulation of key enzymes, such as ACACA/ACACB, fatty-acyl-CoA elongation enzyme and dihydroceramide desaturase, and defective PI3K/Akt and calcium signaling pathways indicate drastic changes in cellular energy metabolism and redox regulation following chronic UV exposure. These metabolic alterations suggest that lipid pathway disruption is a may represent an important mechanism in UV-induced photoaging and reveal novel targets for the treatment of pigmentary diseases. Identification of metabolic chokepoints for fatty acid and sphingolipid production could guide the design of lipid-targeted therapies to prevent and treat SL.

Notwithstanding these significant findings regarding lipid metabolic dysregulation in SL, several inherent study constraints require careful consideration. The relatively small sample size (n = 7 pairs) may limit the generalizability of these results to broader populations with SL. Additionally, our conclusions are primarily derived from transcriptomic data and computational modeling approaches. Direct experimental validation through targeted metabolic profiling or functional biochemical assays would substantially strengthen the mechanistic interpretations presented. Nevertheless, the consistent patterns observed across multiple metabolic pathways suggest robust detection of major pathway alterations. Future research employing larger cohorts with experimental validation will be essential to validate these findings and to examine lipid-targeted therapeutic strategies in clinical dermatology.

## Data availability statement

The datasets presented in this study can be found in online repositories. The names of the repository/repositories and accession

number(s) can be found below: NCBI Gene Expression Omnibus (GEO), GSE318414 <https://www.ncbi.nlm.nih.gov/geo/query/acc.cgi?acc=GSE318414>.

## Ethics statement

The studies involving humans were approved by Institutional Review Board of Kyung Hee University Hospital at Gangdong 494 (KHNMC 2022-04-014). The studies were conducted in accordance with the local legislation and institutional requirements. The participants provided their written informed consent to participate in this study.

## Author contributions

SK: Methodology, Investigation, Writing – original draft, Formal Analysis. WL: Formal Analysis, Methodology, Writing – original draft, Investigation. JK: Visualization, Writing – original draft, Software. YL: Writing – original draft, Software. KL: Writing – original draft, Visualization. MK: Investigation, Conceptualization, Writing – original draft, Writing – review and editing, Supervision. S-HK: Resources, Conceptualization, Writing – review and editing, Investigation, Supervision, Writing – original draft.

## Funding

The author(s) declared that financial support was received for this work and/or its publication. This work was supported by a grant of the Korea Health Technology R&D Project grant through the Korea Health Industry Development Institute (KHIDI), funded by the Ministry of Health & Welfare, Republic of Korea (grant number: RS-2023-KH141370) and by Global - Learning & Academic research institution for Master's-PhD students, and Postdocs (G-LAMP) Program of the National Research Foundation of Korea (NRF) grant funded by the Ministry of Education (No. RS-2025-25442355).

## Conflict of interest

The author(s) declared that this work was conducted in the absence of any commercial or financial relationships that could be construed as a potential conflict of interest.

## Generative AI statement

The author(s) declared that generative AI was not used in the creation of this manuscript.

Any alternative text (alt text) provided alongside figures in this article has been generated by Frontiers with the support of artificial intelligence and reasonable efforts have been made to

ensure accuracy, including review by the authors wherever possible. If you identify any issues, please contact us.

## Publisher's note

All claims expressed in this article are solely those of the authors and do not necessarily represent those of their affiliated organizations, or those of the publisher, the editors and the reviewers. Any product that may be evaluated in this article, or claim that may be made by its manufacturer, is not guaranteed or endorsed by the publisher.

## Supplementary material

The Supplementary Material for this article can be found online at: <https://www.frontiersin.org/articles/10.3389/fcell.2026.1751543/full#supplementary-material>

### SUPPLEMENTARY FIGURE S1

Glycerophospholipid metabolism pathway map. KEGG pathway diagram showing comprehensive glycerophospholipid metabolic network with metabolic flux changes in solar lentigo. Color-coded reactions indicate upregulation (red) and downregulation (green) based on constraint-based flux simulation. Key enzymes and intermediates are labeled with KEGG identifiers. This detailed pathway view supports the glycerophospholipid findings presented in Figure 1.

### SUPPLEMENTARY FIGURE S2

Sphingolipid metabolism pathway map. KEGG pathway diagram illustrating complete sphingolipid biosynthetic and catabolic pathways with metabolic flux alterations in solar lentigo lesions. Color scale represents log<sub>2</sub> fold changes in reaction activities, highlighting reduced ceramide synthesis (DHCRD2) and compensatory mechanisms. Pathway includes ceramide,

sphingomyelin, and glycosphingolipid branches supporting Figure 3 analysis.

### SUPPLEMENTARY FIGURE S3

Tyrosine metabolism pathway map. Comprehensive KEGG pathway showing tyrosine catabolism and melanin biosynthesis with metabolic flux changes in solar lentigo. Enhanced tyrosine hydroxylase activity and melanogenesis are evident, while tyrosine degradation pathways show suppression. Color-coded metabolites and reactions support the oxidative stress and melanogenic findings described in Figure 4.

### SUPPLEMENTARY FIGURE S4

Fatty acid biosynthesis pathway map. KEGG pathway diagram displaying fatty acid synthesis and elongation networks with metabolic alterations in solar lentigo. Shows coordinated downregulation of acetyl-CoA carboxylase (ACACA/ACACB) and fatty acid elongation systems. Color-coded pathway components illustrate the systematic suppression of fatty acid metabolism supporting Figure 2 results.

### SUPPLEMENTARY FIGURE S5

Primary bile acid biosynthesis pathway map. KEGG pathway showing cholesterol-to-bile acid conversion with metabolic flux changes in solar lentigo. Demonstrates coordinated suppression of key enzymes including CYP27A1, AMACR, and related hydroxylases. Color gradient indicates reduced bile acid production capacity, supporting the cholesterol turnover disruption described in Figure 6.

### SUPPLEMENTARY FIGURE S6

Cholesterol metabolism pathway map. Comprehensive KEGG pathway diagram of cholesterol biosynthesis from acetyl-CoA with metabolic flux alterations in solar lentigo. Shows systematic downregulation of mevalonate pathway enzymes, squalene synthesis, and sterol ring formation. Color-coded reactions demonstrate the coordinated suppression of cholesterol biosynthesis presented in Figure 7.

### SUPPLEMENTARY FIGURE S7

Inositol phosphate metabolism pathway map. KEGG pathway illustrating inositol phosphate signaling networks and phosphatidylinositol metabolism with flux changes in solar lentigo. Highlights PTEN-mediated PI3K/AKT pathway disruption and calcium signaling alterations. Color-coded metabolites show reduced PIP3 phosphatase activity and altered second messenger systems supporting Figure 5 findings.

## References

- Aoki, H., Moro, O., Tagami, H., and Kishimoto, J. (2007). Gene expression profiling analysis of solar lentigo in relation to immunohistochemical characteristics. *Br. J. Dermatol.* 156 (6), 1214–1223. doi:10.1111/j.1365-2133.2007.07830.x
- Bastiaens, M., Hoefnagel, J., Westendorp, R., Vermeer, B. J., and Bouwes Bavinck, J. N. (2004). Solar lentigines are strongly related to sun exposure in contrast to ephelides. *Pigment. Cell Res.* 17 (3), 225–229. doi:10.1111/j.1600-0749.2004.00131.x
- Batagov, A., Dalan, R., Wu, A., Lai, W., Tan, C. S., and Eisenhaber, F. (2023). Generalized metabolic flux analysis framework provides mechanism-based predictions of ophthalmic complications in type 2 diabetes patients. *Health Inf. Sci. Syst.* 11 (1), 18. doi:10.1007/s13755-023-00218-x
- Bowman, C. E., and Wolfgang, M. J. (2019). Role of the malonyl-CoA synthetase ACSF3 in mitochondrial metabolism. *Adv. Biol. Regul.* 71, 34–40. doi:10.1016/j.jbior.2018.09.002
- Cai, D., Zhang, H., Zhang, C., Xiao, X., Cui, X., Gu, X., et al. (2025). Dynamic network driver analysis identifies master factors associated with progression of solar lentigines. *Biol. (Basel).* 14 (7), 876. doi:10.3390/biology14070876
- Chen, J., Huang, L., Quan, J., and Xiang, D. (2021). TRIM14 regulates melanoma malignancy via PTEN/PI3K/AKT and STAT3 pathways. *Aging* 13 (9), 13225–13238. doi:10.18632/aging.203003
- Chen, J., Yin, Z., Yu, N., Ou, S., Wang, X., Li, H., et al. (2024). Tanshinone alleviates UVA-induced melanogenesis in melanocytes via the Nrf2-regulated antioxidant defense signaling pathway. *Curr. Mol. Med.* 24 (12), 1529–1539. doi:10.2174/0115665240263196230920161019
- Chen, X., Ouyang, L., Jia, S., and Zhao, M. (2024). Oxysterols contribute to immune cell recruitment in SLE skin lesions. *Arthritis Res. Ther.* 26 (1), 181. doi:10.1186/s13075-024-03414-6
- Chien, Y., Lai, Y. H., Kwok, C. F., and Ho, L. T. (2011). Endothelin-1 suppresses long-chain fatty acid uptake and glucose uptake via distinct mechanisms in 3T3-L1 adipocytes. *Obesity* 19 (1), 6–12. doi:10.1038/oby.2010.124
- Choi, Y., Nam, U., and Kim, J. (2025). CPT1B-Mediated fatty acid oxidation induces pigmentation in solar lentigo. *Pigment. Cell Melanoma Res.* doi:10.1101/2025.06.15.659823
- Coelho, S. G., Valencia, J. C., Yin, L., Smuda, C., Mahns, A., Kolbe, L., et al. (2015). UV exposure modulates hemidesmosome plasticity, contributing to long-term pigmentation in human skin. *J. Pathol.* 236 (1), 17–29. doi:10.1002/path.4497
- Conde-Perez, A., Gros, G., Longvert, C., Pedersen, M., Petit, V., Aktary, Z., et al. (2015). A caveolin-dependent and PI3K/AKT-independent role of PTEN in  $\beta$ -catenin transcriptional activity. *Nat. Commun.* 6, 8093. doi:10.1038/ncomms9093
- Conner, E. M. (2021). Hydrogen peroxide in cellular signaling and disease. *Antioxid. Redox Signal* 35 (12), 987–1002. doi:10.1089/ars.2020.8176
- da Silva, W. A., Fazelinia, H., Rosenthal, S. B., Laiakis, E. C., Kim, M. S., Meydan, C., et al. (2020). Comprehensive multi-omics analysis reveals mitochondrial stress as a central biological hub for spaceflight impact. *Cell* 183 (5), 1185–1201. doi:10.1016/j.cell.2020.11.002
- Dalmau, N., Andrieu-Abadie, N., Tauler, R., and Bedia, C. (2018). Phenotypic and lipidomic characterization of primary human epidermal keratinocytes exposed to simulated solar UV radiation. *J. Dermatol. Sci.* 92 (1), 97–105. doi:10.1016/j.jdermsci.2018.07.002
- Dini, I., Falanga, D., Di Lorenzo, R., Tito, A., Carotenuto, G., Zappelli, C., et al. (2021). An extract from ficus carica cell cultures works as an anti-stress ingredient for the skin. *Antioxidants* 10 (4), 515. doi:10.3390/antiox10040515
- Downward, J. (2004). PI 3-kinase, akt and cell survival. *Semin. Cell Dev. Biol.* 15 (2), 177–182. doi:10.1016/j.semcdb.2004.01.002
- Duarte, N. C., Becker, S. A., Jamshidi, N., Thiele, I., Mo, M. L., Vo, T. D., et al. (2007). Global reconstruction of the human metabolic network based on genomic and bibliomic data. *Proc. Natl. Acad. Sci. U. S. A.* 104 (6), 1777–1782. doi:10.1073/pnas.0610772104
- Ewald, D. A., Malajian, D., Krueger, J. G., Workman, C. T., Wang, T., Tian, S., et al. (2015). Meta-analysis derived atopic dermatitis (MADAD) transcriptome defines a robust AD signature highlighting the involvement of atherosclerosis and lipid metabolism pathways. *BMC Med. Genomics* 8, 1–15. doi:10.1186/s12920-015-0133-x

- Fabrias, G., Muñoz-Olaya, J., Cingolani, F., Signorelli, P., Casas, J., Gagliostro, V., et al. (2012). Dihydroceramide desaturase and dihydroshingolipids: debutant players in the sphingolipid arena. *Prog. Lipid Res.* 51 (2), 82–94. doi:10.1016/j.plipres.2011.12.002
- Goyarts, E., Muizzuddin, N., Maes, D., and Giacomoni, P. U. (2007). Morphological changes associated with aging: age spots and the microinflammatory model of skin aging. *Ann. N. Y. Acad. Sci.* 1119 (1), 32–39. doi:10.1196/annals.1404.006
- Guarnieri, J. W., Dybas, J. M., Fazelinia, H., Kim, M. S., Frere, J., Zhang, Y., et al. (2023). Core mitochondrial genes are down-regulated during SARS-CoV-2 infection of rodent and human hosts. *Sci. Transl. Med.* 15 (708), eabq1533. doi:10.1126/scitranslmed.abq1533
- Imokawa, G. (2019). Melanocyte activation mechanisms and rational therapeutic treatments of solar lentigos. *Int. J. Mol. Sci.* 20 (15), 3666. doi:10.3390/ijms20153666
- Iyengar, B., and Misra, R. S. (1987). Reaction of dendritic melanocytes in vitiligo to the substrates of tyrosine metabolism. *Cells Tissues Organs* 129 (3), 203–205. doi:10.1159/000146400
- Jenkins, N. C., Liu, T., Cassidy, P., Leachman, S. A., Boucher, K. M., Goodson, A. G., et al. (2013). The p16INK4A tumor suppressor regulates cellular oxidative stress. *Oncogene* 32 (25), 3063–3068. doi:10.1038/ncr.2012.325
- Jeong, J., Lee, W., Kim, Y. A., Lee, Y. J., Kim, S., Shin, J., et al. (2024). Multi-system-level analysis reveals differential expression of stress response-associated genes in inflammatory solar lentigo. *Int. J. Mol. Sci.* 25 (7), 3973. doi:10.3390/ijms25073973
- Kang, H. Y., Suzuki, I., Lee, D. J., Ha, J., Reiniche, P., Aubert, J., et al. (2011). Transcriptional profiling shows altered expression of wnt Pathway and lipid metabolism-related genes as well as melanogenesis-related genes in melasma. *J. Invest. Dermatol.* 131 (8), 1692–1700. doi:10.1038/jid.2011.109
- Kim, N. H., and Lee, A. Y. (2023). Oxidative stress induces skin pigmentation in melasma by inhibiting hedgehog signaling. *Antioxidants* 12 (11), 1969. doi:10.3390/antiox12111969
- Kim, K., Yoon, J., and Lim, K. M. (2024). Syringaresinol attenuates  $\alpha$ -melanocyte-stimulating hormone-induced reactive oxygen species generation and melanogenesis. *Antioxidants* 13 (7), 876. doi:10.3390/antiox13070876
- Korotkevich, G., Sukhov, V., Budin, N., Shpak, B., Artyomov, M. N., and Sergushichev, A. (2016). Fast gene set enrichment analysis. *bioRxiv*, 060012. doi:10.1101/060012
- Kumar, S., Yadav, D. K., Choi, E. H., and Kim, M. H. (2018). Insight from molecular dynamic simulation of reactive oxygen species in oxidized skin membrane. *Sci. Rep.* 8 (1), 13271. doi:10.1038/s41598-018-31609-w
- Lee, Y. J., Kim, W. I., Park, T. H., Bae, J. H., Nam, H. S., Cho, S. W., et al. (2021). Upregulation of DJ-1 expression in melanoma regulates PTEN/AKT pathway for cell survival and migration. *Arch. Dermatol. Res.* 313 (7), 583–591. doi:10.1007/s00403-020-02139-1
- Li, Z. Y., Chang, S. H., Liu, K. T., Wu, A. E., Hsu, C. S., Huang, S. W., et al. (2024). Low-dose imiquimod induces melanogenesis in melanoma cells through an ROS-mediated pathway. *J. Dermatol. Sci.* 113 (1), 18–25. doi:10.1016/j.jdermsci.2023.12.005
- Li, C. Y., Wang, W. T., Ma, S. H., Lo, L. W., Wu, C. Y., Chang, W. C., et al. (2025). Association of proprotein convertase subtilisin/kexin type-9 inhibitors with risk of nonmelanoma skin cancer: a retrospective cohort study. *Br. J. Dermatol.* 192 (4), 697–705. doi:10.1093/bjd/ljae438
- Liu, S., Liu, F., Zhang, Z., Zhuang, Z., Yuan, X., and Chen, Y. (2023). The SELP, CD93, IL2RG, and VAV1 genes associated with atherosclerosis may be potential diagnostic biomarkers for psoriasis. *J. Inflamm. Res.* 16, 827–843. doi:10.2147/JIR.S398862
- Łuczaj, W., Domingues, M. D. R., Domingues, P., and Skrzydlewska, E. (2020). Changes in lipid profile of keratinocytes from rat skin exposed to chronic UVA or UVB radiation and topical application of cannabidiol. *Antioxidants* 9 (12), 1178. doi:10.3390/antiox9121178
- Luo, R., Zheng, Z., Yang, C., Zhang, X., Cheng, L., Su, G., et al. (2020). Comparative transcriptome analysis provides insights into the polyunsaturated fatty acid synthesis regulation of Fat-1 transgenic sheep. *Int. J. Mol. Sci.* 21 (3), 1121. doi:10.3390/ijms21031121
- Luo, L., Yu, X., Zeng, H., Hu, Y., Jiang, L., Huang, J., et al. (2023a). Fraxin inhibits melanogenesis by suppressing the ERK/MAPK pathway and antagonizes oxidative stress by activating the NRF2 pathway. *Heliyon* 9 (8), e18929. doi:10.1016/j.heliyon.2023.e18929
- Luo, L., Jia, W., Zhang, Y., Guo, Y., Zhu, J., and Li, C. (2023b). Proprotein convertase furin regulates melanogenesis via the notch signaling pathway. *Discov. Med.* 35 (175), 144–156. doi:10.24976/Discov.Med.202335175.15
- Ma, X., Lu, L., Zhao, Z., Cai, M., Gao, N., and Han, G. (2020). Lipidomics profiling of skin surface lipids in senile pruritus. *Lipids Health Dis.* 19 (1), 171. doi:10.1186/s12944-020-01347-y
- Meyer, J. M., Lee, E., Celli, A., Park, K., Cho, R., Lambert, W., et al. (2021). CERKL is upregulated in cutaneous squamous cell carcinoma and maintains cellular sphingolipids and resistance to oxidative stress. *Br. J. Dermatol.* 185 (1), 147–152. doi:10.1111/bjd.19753
- Motokawa, T., Kato, T., Katagiri, T., Matsunaga, J., Takeuchi, I., Tomita, Y., et al. (2005). Messenger RNA levels of melanogenesis-associated genes in lentigo senilis lesions. *J. Dermatol. Sci.* 37 (2), 120–123. doi:10.1016/j.jdermsci.2004.10.009
- Muresan, X. M., Narzt, M. S., Woodby, B., Ferrara, F., Gruber, F., and Valacchi, G. (2019). Involvement of cutaneous SR-B1 in skin lipid homeostasis. *Arch. Biochem. Biophys.* 666, 1–7. doi:10.1016/j.abb.2019.03.005
- Namiki, T., Yaguchi, T., Nakamura, K., Valencia, J. C., Coelho, S. G., Yin, L., et al. (2015). NUA2 amplification coupled with PTEN deficiency promotes melanoma development via CDK activation. *Cancer Res.* 75 (13), 2708–2715. doi:10.1158/0008-5472.CAN-13-3209
- Ntambi, J. M. (1999). Regulation of stearyl-CoA desaturase by polyunsaturated fatty acids and cholesterol. *J. Lipid Res.* 40 (9), 1549–1558. doi:10.1016/S0022-2275(20)33401-5
- Oh, J. H., Hur, W., Li, N., and Jo, S. J. (2022). Effects of the epidermal growth factor receptor inhibitor, gefitinib, on lipid and hyaluronic acid synthesis in cultured HaCaT keratinocytes. *Exp. Dermatol.* 31 (6), 918–927. doi:10.1111/exd.14538
- Padyana, A. K., Gross, S., Jin, L., Cianchetta, G., Narayanaswamy, R., Wang, F., et al. (2019). Structure and inhibition mechanism of the catalytic domain of human squalene epoxidase. *Nat. Commun.* 10 (1), 97. doi:10.1038/s41467-018-07928-x
- Papaccio, F., Ottaviani, M., Truglio, M., D'Arino, A., Caputo, S., Pacifico, A., et al. (2024). Markers of metabolic abnormalities in vitiligo patients. *Int. J. Mol. Sci.* 25 (18), 10201. doi:10.3390/ijms251810201
- Patra, V., Bordag, N., Clement, Y., Köfeler, H., Nicolas, J. F., Vocanson, M., et al. (2023). Ultraviolet exposure regulates skin metabolome based on the microbiome. *Sci. Rep.* 13 (1), 7207. doi:10.1038/s41598-023-34073-3
- Pietrzak, A., Michalak-Stoma, A., Chodorowska, G., and Szepietowski, J. C. (2010). Lipid disturbances in psoriasis: an update. *Mediat. Inflamm.* 2010 (1), 535612. doi:10.1155/2010/535612
- Scortegagna, M., Lau, E., Zhang, T., Feng, Y., Sereduk, C., Yin, H., et al. (2015). PDK1 and SGK3 contribute to the growth of BRAF-mutant melanomas and are potential therapeutic targets. *Cancer Res.* 75 (7), 1399–1412. doi:10.1158/0008-5472.CAN-14-2785
- Shannon, P., Markiel, A., Ozier, O., Baliga, N. S., Wang, J. T., Ramage, D., et al. (2003). Cytoscape: a software environment for integrated models of biomolecular interaction networks. *Genome Res.* 13 (11), 2498–2504. doi:10.1101/gr.1239303
- Smith, A. C., and Robinson, A. J. (2011). A metabolic model of the mitochondrion and its use in modelling diseases of the tricarboxylic acid cycle. *BMC Syst. Biol.* 5, 1–13. doi:10.1186/1752-0509-5-102
- Speeckaert, R., Bulat, V., Speeckaert, M. M., and van Geel, N. (2023). The impact of antioxidants on vitiligo and melasma: a scoping review and meta-analysis. *Antioxidants* 12 (12), 2082. doi:10.3390/antiox12122082
- Sun, H., Meng, Y., Yao, L., Du, S., Li, Y., Zhou, Q., et al. (2024). Ubiquitin-specific protease 22 controls melanoma metastasis and vulnerability to ferroptosis through targeting SIRT1/PTEN/PI3K signaling. *MedComm* 5 (8), e684. doi:10.1002/mco2.684
- Szklarczyk, D., Kirsch, R., Koutrouli, M., Nastou, K., Mehryary, F., Hachilif, R., et al. (2023). The STRING database in 2023: protein-protein association networks and functional enrichment analyses for any sequenced genome of interest. *Nucleic Acids Res.* 51 (D1), D638–D646. doi:10.1093/nar/gkac1000
- Tessema, E. N., Gebre-Mariam, T., Paulos, G., Wohlrab, J., and Neubert, R. H. H. (2018). Delivery of oat-derived phytoceramide into the stratum corneum of the skin using nanocarriers: formulation, characterization and *in vitro* and *ex-vivo* penetration studies. *Eur. J. Pharm. Biopharm.* 127, 260–269. doi:10.1016/j.ejpb.2018.02.037
- Trakaki, A., and Marsche, G. (2020). High-density lipoprotein (HDL) in allergy and skin diseases: focus on immunomodulating functions. *Biomedicines* 8 (12), 558. doi:10.3390/biomedicines8120558
- Tu, Y., Gu, H., Li, N., Sun, D., Yang, Z., and He, L. (2024). Identification of key genes related to immune-lipid metabolism in skin barrier damage and analysis of immune infiltration. *Inflammation* 48, 2051–2068. doi:10.1007/s10753-024-02174-4
- Vecchio, L. M., Moura, A. L., and Silva, C. R. (2021). Tyrosine metabolism and oxidative stress in pigmented disorders. *J. Dermatol. Res.* 8 (3), 245–258. doi:10.1007/s40200-021-00785-4
- Wang, H., Humatova, A., Liu, Y., Qin, W., Lee, M., Cesarato, N., et al. (2020). Mutations in SREBF1, encoding sterol regulatory element binding transcription factor 1, cause autosomal-dominant IFAP syndrome. *Am. J. Hum. Genet.* 107 (1), 34–45. doi:10.1016/j.ajhg.2020.05.006
- Wang, Y., Lan, Y., Yang, X., Gu, Y., and Lu, H. (2021). TGF $\beta$ 2 upregulates tyrosinase activity through opsin-3 in human skin melanocytes *in vitro*. *J. Invest. Dermatol.* 141 (11), 2679–2689. doi:10.1016/j.jid.2021.01.040
- Wu, J., and Zhao, H. (2024). Role of SIRPG gene in type 1 diabetes and lichen planus. *Medicine* 103 (45), e40454. doi:10.1097/MD.00000000000040454
- Wu, T., Hu, E., Xu, S., Chen, M., Guo, P., Dai, Z., et al. (2021). clusterProfiler 4.0: a universal enrichment tool for interpreting omics data. *Innovation* 2 (3), 100141. doi:10.1016/j.xinn.2021.100141
- Yonei, N., Kaminaka, C., Kimura, A., Furukawa, F., and Yamamoto, Y. (2012). Two patterns of solar lentigines: a histopathological analysis of 40 Japanese women. *J. Dermatol.* 39 (10), 829–832. doi:10.1111/j.1346-8138.2012.01574.x
- Yu, X., Liu, S., Li, Y., and Yuan, S. (2024). Molecular insights into the penetration enhancement mechanism of terpenes to skin. *J. Phys. Chem. B* 128 (50), 12507–12516. doi:10.1021/acs.jpcc.4c05910
- Zhu, Y., Xu, J., Song, X., and Xiang, W. (2024). Comparative study of melasma in patients before and after treatment based on lipomics. *Lipids Health Dis.* 23 (1), 138. doi:10.1186/s12944-024-02130-z

## Glossary

<b>ACACA</b>	Acetyl-CoA carboxylase alpha	<b>MVK</b>	Mevalonate kinase
<b>ACACB</b>	Acetyl-CoA carboxylase beta	<b>PAFAH2</b>	Platelet activating factor acetylhydrolase 2
<b>ACAT2</b>	Acetyl-CoA acetyltransferase 2	<b>PC</b>	Phosphatidylcholine
<b>ACSBG1</b>	Acyl-CoA synthetase bubblegum family member 1	<b>PE</b>	Phosphatidylethanolamine
<b>ACSL5</b>	Acyl-CoA synthetase long-chain family member 5	<b>PIP<sub>2</sub></b>	Phosphatidylinositol 4,5-bisphosphate
<b>AMACR</b>	Alpha-methylacyl-CoA racemase	<b>PIP<sub>3</sub></b>	Phosphatidylinositol 3,4,5-trisphosphate
<b>APOA1</b>	Apolipoprotein A1	<b>PLA2G7</b>	Phospholipase A2 group VII
<b>CH25H</b>	Cholesterol 25-hydroxylase	<b>PLCB3</b>	Phospholipase C beta 3
<b>COMTD1</b>	Catechol-O-methyltransferase domain containing 1	<b>PLCH2</b>	Phospholipase C eta 2
<b>CYP27A1</b>	Cytochrome P450 family 27 subfamily A member 1	<b>PMVK</b>	Phosphomevalonate kinase
<b>DAG</b>	Diacylglycerol	<b>PPI</b>	Protein-protein interaction
<b>DEGS1</b>	Delta 4-desaturase, sphingolipid 1	<b>PS</b>	Phosphatidylserine
<b>DEGS2</b>	Delta 4-desaturase, sphingolipid 2	<b>PTEN</b>	Phosphatase and tensin homolog
<b>DHCR7</b>	7-dehydrocholesterol reductase	<b>PTDSS1</b>	Phosphatidylserine synthase 1
<b>DHCR24</b>	24-dehydrocholesterol reductase	<b>ROS</b>	Reactive oxygen species
<b>DGKQ</b>	Diacylglycerol kinase theta	<b>SL</b>	Solar lentigo
<b>DUOX2</b>	Dual oxidase 2	<b>SMPD3</b>	Sphingomyelin phosphodiesterase 3
<b>EC</b>	Enzyme Commission	<b>SQLE</b>	Squalene epoxidase
<b>ELOVL4</b>	ELOVL fatty acid elongase 4	<b>STRING</b>	Search Tool for the Retrieval of Interacting Genes/Proteins
<b>FDR</b>	False discovery rate	<b>TH</b>	Tyrosine hydroxylase
<b>GO</b>	Gene Ontology	<b>TM7SF2</b>	Transmembrane 7 superfamily member 2
<b>GSEA</b>	Gene Set Enrichment Analysis	<b>TPM</b>	Transcripts per million
<b>HDL</b>	High-density lipoprotein	<b>UGCG</b>	UDP-glucose ceramide glucosyltransferase
<b>HSD17B4</b>	Hydroxysteroid 17-beta dehydrogenase 4	<b>UV</b>	Ultraviolet
<b>INPP5E</b>	Inositol polyphosphate-5-phosphatase E		
<b>IP<sub>3</sub></b>	Inositol 1,4,5-trisphosphate		
<b>IRB</b>	Institutional Review Board		
<b>ITPKC</b>	Inositol-trisphosphate 3-kinase C		
<b>KEGG</b>	Kyoto Encyclopedia of Genes and Genomes		
<b>LDL</b>	Low-density lipoprotein		
<b>LDLR</b>	Low-density lipoprotein receptor		
<b>LRP1</b>	LDL receptor related protein 1		
<b>LRP2</b>	LDL receptor related protein 2		